γ-Fe$_2$O$_3$ AND γ-Fe$_2$O$_3$-TiO$_2$ ULTRAFINE PARTICLE FILMS AS REDUCING GAS SENSOR

N. REZLESCU, C. DOROFTEI, E. REZLESCU, M. L. CRAUS

Institute of Technical Physics, Bld. D. Mangeron 47, 700050 Iasi, Romania, reznic@phys-iasi.ro

Abstract. In this paper, the preparation of γ-Fe$_2$O$_3$ and γ-Fe$_2$O$_3$-TiO$_2$ thick films by screen printing method is presented and their sensitivities and selectivities to acetone, ethyl alcohol, ammonia and LPG are studied. The experimental results revealed that the gas sensitivity is strongly related to operating temperature, film composition and gas type.

Key words: ferric oxide, gas sensor, substitution, sol-gel-selfcombustion.

1. INTRODUCTION

Many different semiconducting oxides in bulk ceramic [1–4], thick film [5, 6] and thin film [7–11] form have been studied as candidate sensor element for reducing gases. The sensing mechanism of the gases is based on changes in surface conductivity induced by chemical reaction between target gases and oxygen adsorbed onto the metal oxide surface [12, 13]. The gas-sensor reaction occurs at elevated temperatures (150–600°C). Recently, Martins *et al.* [14] reported about an ozone sensor working at room temperature. The effect observed upon exposure to reducing gases is a drop in the bulk resistance of the sensor element. The sensitivity of the gas sensor has been shown to increase with decreasing grain size [11]; therefore nanocrystalline metal oxides are expected to exhibit high sensitivity.

Thick film technology offers certain advantages in the construction of gas sensors. The manufacturing technology can be made reproducible. Also, a heater as well as a temperature sensor can be integrated within sensor construction.

In this study, two thick films, γ-Fe$_2$O$_3$ and γ-Fe$_2$O$_3$ - TiO$_2$, were fabricated and their sensitivities and selectivities to acetone, ethyl alcohol (ethanol), ammonia and liquefied petroleum gas (LPG) were studied. γ-Fe$_2$O$_3$ is a n-type semiconductor in which adsorbed oxygen can react with a reducing gas releasing electrons into the conduction band. Because γ-Fe$_2$O$_3$ behaves as a n-type semiconductor, its conductivity will increase after exposure to reducing gases.

TiO$_2$ can modify the intrinsic physical properties of γ-Fe$_2$O$_3$, such as: a) the electrical transport properties by introduction of new states in the band structure of γ-Fe$_2$O$_3$; b) the surface morphology which has an important role in the chemical reactions between oxide and gas; c) the grain size distribution which contributes in determining the electrical resistance of the material.

The interaction between the gas molecules and the surface of the sensing film depends on its morphologic structure [15]. The surface morphology of the films was analysed using a scanning electron microscope.

2. EXPERIMENTAL

Two thick films of ultrafine particles were prepared by screen printing technology: γ-Fe$_2$O$_3$ and γ-Fe$_2$O$_3$ (66.6 wt%)-TiO$_2$ (33.3 wt%). The γ-Fe$_2$O$_3$ fine powder was prepared in our laboratory by thermal decomposition of ferric oxalate. Reagent grade TiO$_2$ (anatase, 99.9% pure) with average particle size of 0.3 μm was used. Every film composition was ball milled for 20 hours using distiled water (the proportion water:powder was 2:1), to make a homogeneous slurry. The resulting pastes were screen printed on one side of the glass substrates (25 mm / 18 mm / 1 mm) that had printed two silver electrodes, as in Fig. 1. To obtain a good adherence of the film to the glass, a light polishing of the glass substrate with Al$_2$O$_3$ paste was made before the screen printing process. The as obtained thick films were dried at 70°C for 2 hours. Finally, the films were annealed at 400°C, in air, for 1 hour. Thereby, craks free and perfectly adherent films, of about 20 μm thickness were obtained. For gas sensing measurements, the films were introduced in a test chamber and exposed to acetone (CH$_3$COCH$_3$), ammonia (NH$_3$), liquefied petroleum gas (LPG) and ethyl alcohol (C$_2$H$_5$OH) vapor at temperatures above 200°C to promote chemical reaction between test gas and sensor element. The test gases were injected in the test chamber by high precision syringes. A heater
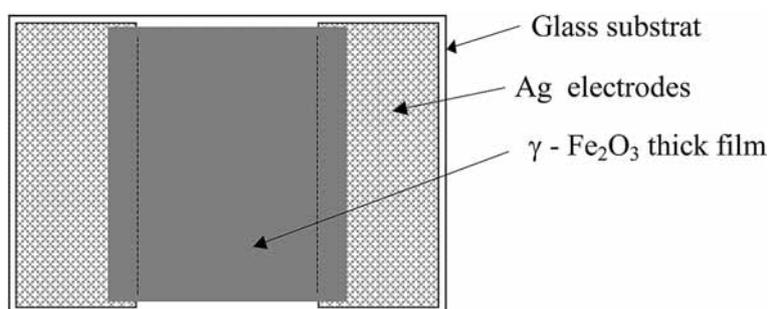

Fig. 1 – Pattern of thick film sensor with silver electrodes.

element was placed in contact with the other face of the glass substrate. A cromel-alumel thermocouple located in close proximity of the sensor element measures the operating temperature.

When the assemble heater-sensor was introduced into the measuring chamber, the resistance of the thick film was measured by two point method, using a digital LCR meter, at 100 Hz, at fixed operating temperatures, from 200 to 350°C, both in air (R_a) and in the presence of a reducing gas (R_g). The sensitivity of the thick film sensor was calculated as the ratio

$$S = \frac{\Delta R}{R_a} = \frac{R_a - R_g}{R_a}.$$

Taking into account the thermal inertia of ceramics, all measurements were carried out under the ferrite thermal stabilization conditions. After each change of the test gas, the sensor element was subjected to heat cleaning at 400°C in order to be activated, that is to form the initial structure and to thermodynamically stabilize it. All the experiments were performed with the test gas concentration of 150 ppm and some others mentioned.

XRD structure analyses were performed with a DRON-2 diffractometer using CoKα radiation. The surface microstructure of the thick films was examined using scanning electron microscope (TESLA BS 340). In order to obtain high resolution SEM pictures, the films were coated with an ultra thin silver layer of 5 nm. The micrographs were taken with 25 kV primary electron beam. Two thick films were produced for each composition, but only one is given in this work. The other film showed the same behavior of the electrical and morphological properties as the one given here.

3. RESULTS AND DISCUSSION

3.1. STRUCTURE

Fig. 2 shows the XRD patterns of γ-Fe₂O₃ and γ-Fe₂O₃ -TiO₂ heat treated at 400°C. XRD patterns reveal that the first sample (Fig. 2a) is a mixture of two phases, maghemite M (γ-Fe₂O₃) and hematite H (α-Fe₂O₃). This means that a phase transition from spinel structure (γ-Fe₂O₃) to corundum structure (α-Fe₂O₃) occurs by firing at 400°C in agreement with [16]. The second sample (Fig.2b) is a mixture of three phases: γ-Fe₂O₃, α-Fe₂O₃ and anatase (A)-type TiO₂ phase.

From XRD data permited to obtain the lattice parameters, average size of the crystalline blocks and microstrains (Table 1). Table 1 reveals that the both samples have a nanogranular structure and the average size of crystalline blocks decreases
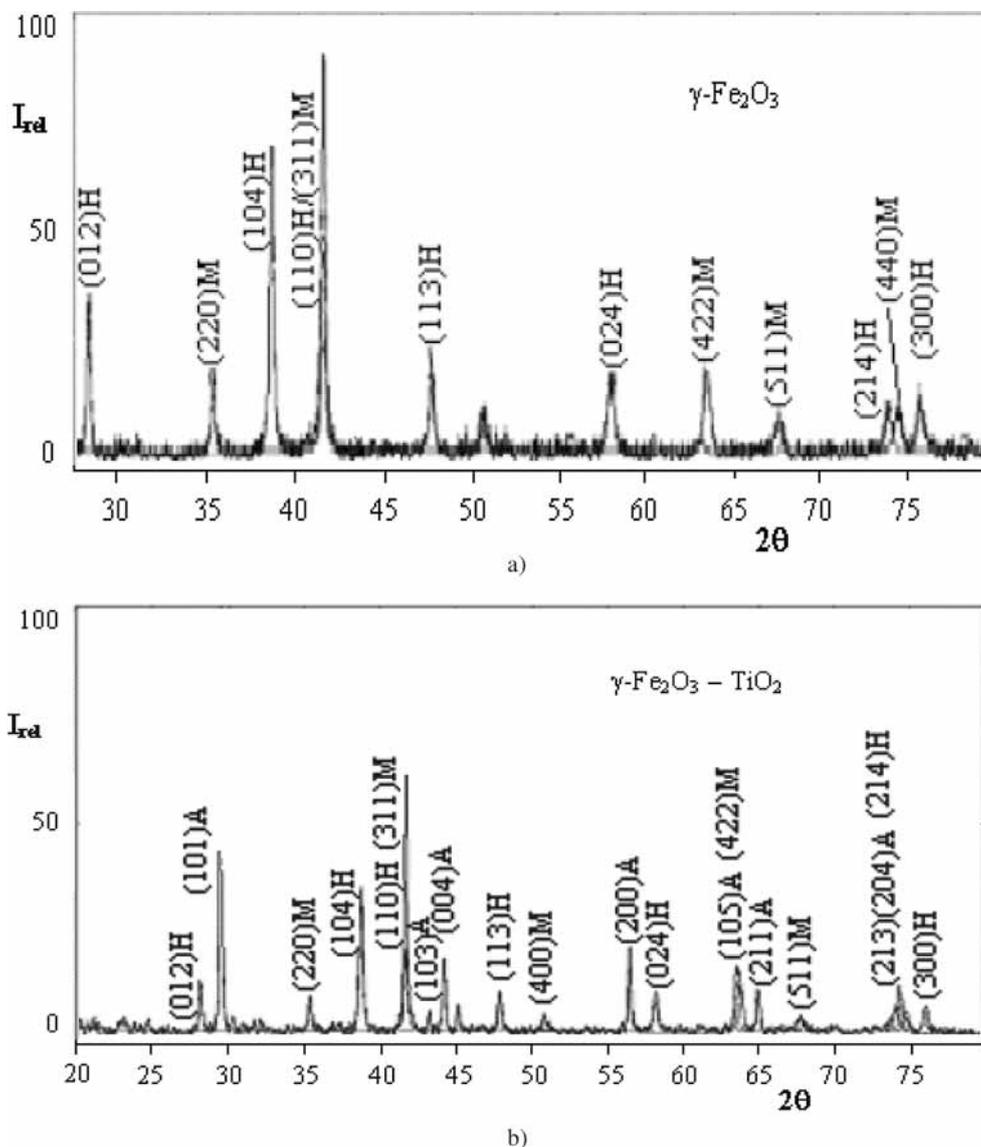
Fig. 2 – XRD patterns of γ-Fe$_2$O$_3$ (a) and γ-Fe$_2$O$_3$-TiO$_2$ (b) after heat treatment at 400°C, for 1 hour
(M – maghemite, H – hematite, A – anatase).

by adding TiO$_2$ to γ-Fe$_2$O$_3$. In agreement to Collyer *et al.* [17], part of octahedral Fe^{3+} ions ($r_{Fe}^{3+} = 0.785$ Å) from the spinel structure of maghemite can be substituted by Ti ions ($r_{Ti}^{4+} = 0.745$ Å). The presence of Ti^{4+} ions on octahedral sites in maghemite leads to a decrease of the microstrains and of the average size of crystalline blocks.

Table 1

Phase composition, lattice constants (a, b, c), average size of the crystalline blocks (D) and microstrains (Є) of γ-Fe$_2$O$_3$ and γ-Fe$_2$O$_3$-TiO$_2$ samples heat treated at 400°C

Sample	Phase composition	Average size D [nm]	Microstrains Є	Lattice constants [nm]
γ-Fe$_2$O$_3$	Hematite (H)	54.44	0.00314	a = b = 0.50409; c = 1.37701
	Maghemite (M)	129.96	0.00166	a = b = c = 0.83426
γ-Fe$_2$O$_3$ - TiO$_2$	Hematite (H)	38.61	0.002298	a = b = 0.50356; c = 1.37468
	Maghemite (M)	76.29	0.001448	a = b = c = 0.83434
	Anatase (A)	97.92	0.000971	a = b = 0.37867; c = 0.95142

The SEM analysis allowed us to study the morphology of the films which has an important role in the gas sensing mechanism. SEM micrographs of the two films are given in Fig. 3. These were made before exposure to test gases. The samples have similar morphology and the occurrence of particle agglomerates was not observed. The micrographs reveal the nanosized structure (grain size about 100 nm) and clearly show that the thick films exhibit an intergranular porosity. Intragranular pores are not observed from SEM observations. The grains are interconnected by necks. The pores are smaller than 100 nm or larger than 100 nm. The ratio of small to large pores increases when TiO$_2$ is present. Also, the γ-Fe$_2$O$_3$-TiO$_2$ thick film is less porous than γ-Fe$_2$O$_3$ film.

3.2. SENSING PROPERTIES

Figs. 4 and 5 highlight the difference in the sensing characteristics of the two thick films to the four reducing gases: ethyl alcohol, acetone, ammonia and LPG. The following observations can be made:

a) the gas sensitivity is strongly related to operating temperature, film composition and gas type;

b) the gas sensitivity increases with increasing temperature and reaches a maximum value at optimum temperature of 310°C for GPL and ethanol gases and 330°C for acetone and ammonia;

c) γ-Fe$_2$O$_3$ ultrafine particle film is more sensitive than γ-Fe$_2$O$_3$-TiO$_2$ ultrafine particle film. The attenuated response of γ-Fe$_2$O$_3$-TiO$_2$ film towards GPL, acetone and ammonia vapours (Fig. 5) is desirable for selective detection of C$_2$H$_5$OH with this sensor.

The sensitivities of the two ultrafine particle films to the four gases are compared in Fig. 6. The sensitivity values correspond to the optimized working temperature for the two sensors. One can see that γ-Fe$_2$O$_3$ film is sensitive to acetone and ethanol (sensitivities of about 60%) and less sensitive to LPG (sensitivity
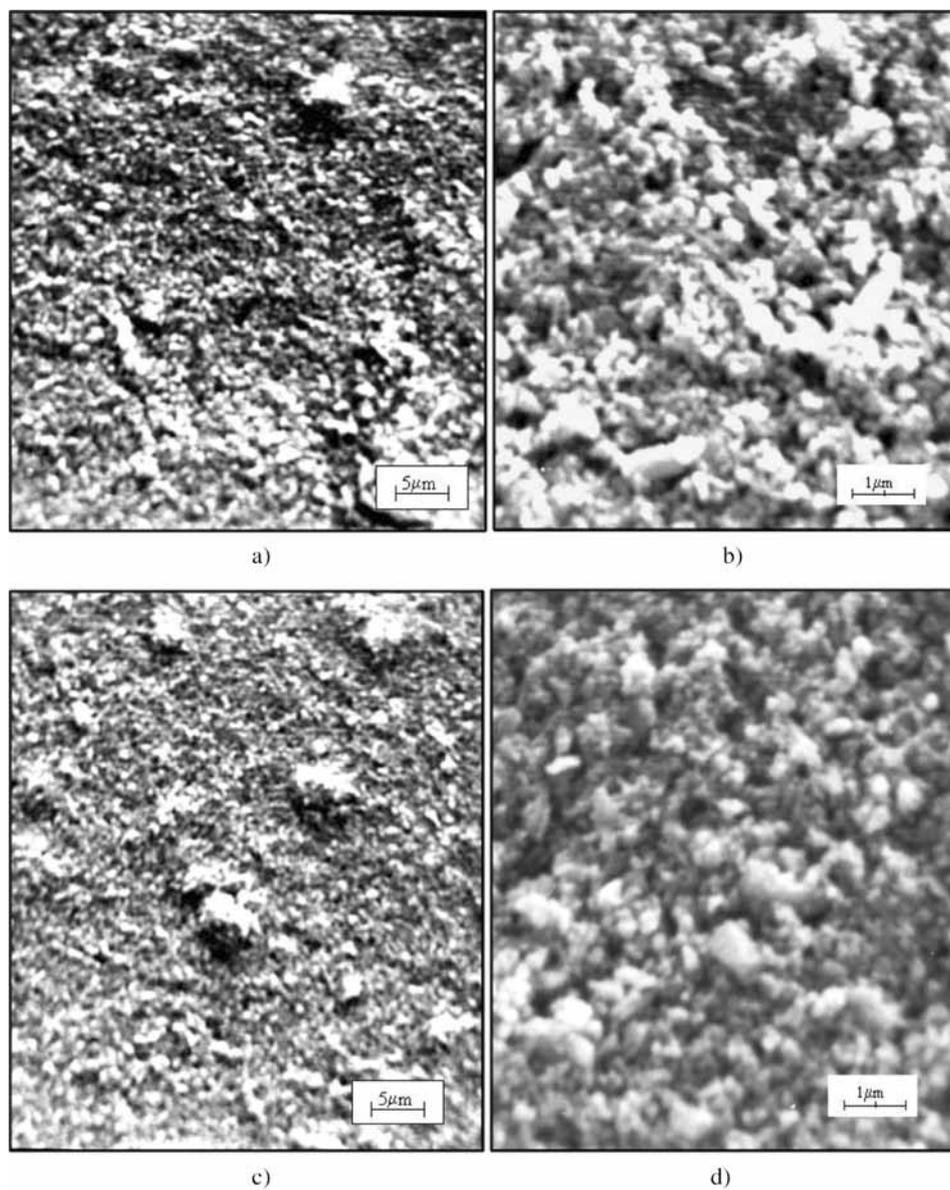
Fig. 3 – SEM micrographs for: a) γ-Fe$_2$O$_3$ (enlargement 1.500); b) γ-Fe$_2$O$_3$ (enlargement 10.000); c) γ-Fe$_2$O$_3$ - TiO$_2$ (enlargement 1.500); d) γ-Fe$_2$O$_3$ -TiO$_2$ (enlargement 10.000).
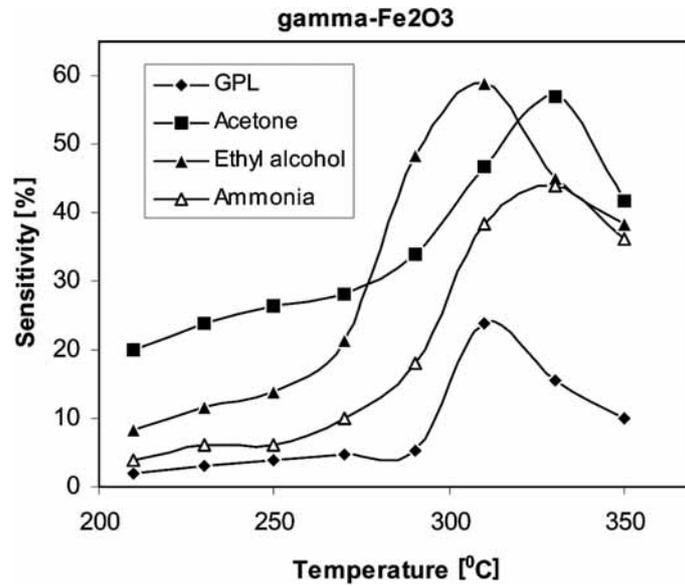
Fig. 4 – Gas sensitivity versus operating temperature for γ-Fe$_2$O$_3$ thick
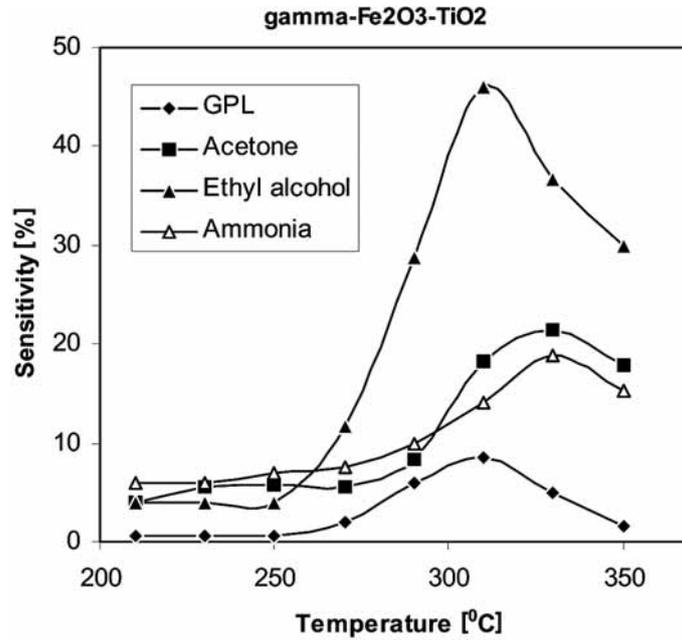film (gas concentration: 150 ppm).

Fig. 5 – Gas sensitivity versus operating temperature for γ-Fe$_2$O$_3$ -TiO$_2$
thick film (gas concentration: 150 ppm).

of about 24%). There is not a large difference between the sensitivities to ethanol and acetone. Also, Fig. 6 clearly indicates that the incorporation of TiO_2 in γ-Fe_2O_3 decreases the sensitivity to test gases, but confers a clear selectivity towards ethanol vapour, mainly due to a decrease of the sensitivity to the other gases. For γ-Fe_2O_3-TiO_2 ultrafine particle film, the sensitivity to ethanol is approximately two times larger than the one under acetone or ammonia, but it is smaller than ethanol sensitivity of γ-Fe_2O_3 ultrafine particle film. The obtained results suggest that the selective sensitivity towards ethanol (C_2H_5OH) of γ-Fe_2O_3-TiO_2 ultrafine particle film can be caused by the involvement of the OH^- hydroxyl group and TiO_2 component. We consider the effect caused by the presence of Ti^{3+} ions in the γ-Fe_2O_3 -TiO_2 film heat treated at 400°C. During the exposure to ethanol, the Ti^{3+} ions are oxidized by hydroxyl groups to form Ti^{4+} ions [18], anion superoxide O^{2-} and molecular hidrogen H_2:

$$2Ti^{3+} + 2OH^- \rightarrow 2Ti^{4+} + 2O^{2-} + H_2,$$

$$O^{2-} \rightarrow \tfrac{1}{2}O_2 + 2\ e^-.$$
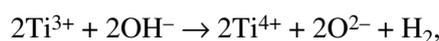
The anion O^{2-} would facilitate the sensor to oxidize immediately the ethanol gas liberating the captured electrons into conduction band.

Yet, γ-Fe_2O_3-TiO_2 thick film is less porous than γ-Fe_2O_3 film and the gas molecules can not freely enter into this film. Therefore, the adsorption of hydroxyl groups is restricted only to the surface of the thick film. Consequently, the sensitivity of γ-Fe_2O_3-TiO_2 to ethanol (about 48%) is smaller as compared to that of the γ-Fe_2O_3 thick film (about 60%), as can see from Fig. 5. Thus, the higher sensitivity of γ-Fe_2O_3 film to the test gases is, probably, the effect of its higher porosity.

However, the results found for sensitivities of the two films indicate that there is another main reason associated with intergranular coupling which can explain the lower sensitivities of γ-Fe_2O_3-TiO_2 ultrafine particle film compared to γ-Fe_2O_3 ultrafine particle film. The experiments show that even if no significant differences in grain size were observed in the two films (Fig. 3), their sensitivities were found to be significantly different. That is, the sensitivity is not controlled by grain size. The intergranular coupling could explain the differences between the gas sensitivities of the two thick films. It has been reported [10] that the gas sensitivity of a film made of particles depends on the overall change of the film conductivity, which results from conductivity changes of all the particles participating in the chemical reaction with the gas detected. The sensitivity will be low if the electrical responses from the individual particles remain isolated.

Therefore, the lower sensitivity of γ-Fe$_2$O$_3$-TiO$_2$ film suggests that there is a poorer intergranular coupling between electrical responses of all the particles due to the presence of the three phases (anatase, maghemite and hematite) having different structures. On the other hand, the enhanced ethanol sensitivity of γ-Fe$_2$O$_3$-TiO$_2$ thick film is the result of the interaction of OH$^-$ group from ethanol with Ti^{3+} ions, as shown above.
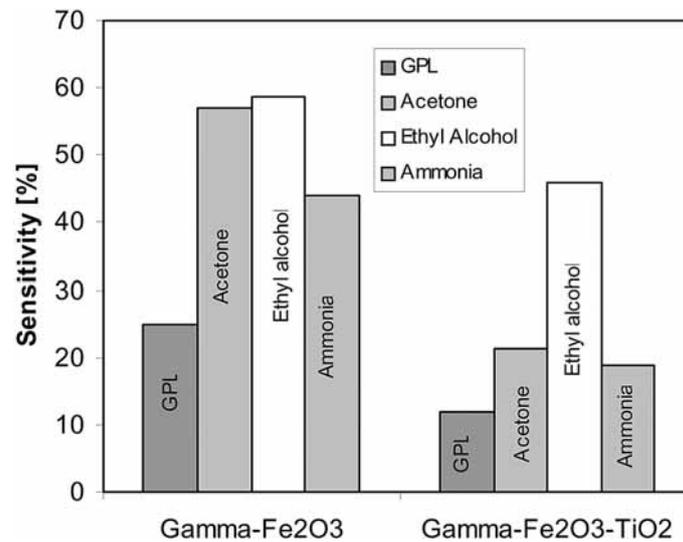
Fig. 6 – Sensitivities of γ-Fe$_2$O$_3$ and γ-Fe$_2$O$_3$-TiO$_2$ thick films to various gases at optimum operating temperatures (gas concentration: 150 ppm).

The variation of the sensitivity of the two thick films has also been investigated as a function of stepwise increasing gas concentration from 0 to 150 ppm. In Fig. 7 (a and b) one can see a sharp increase of the sensitivity upon exposure to low ethanol or acetone concentrations, between 5 and 50 ppm, at operating temperatures of 310°C and 330°C, respectively. For higher concentrations, the sensitivities tend to a saturation value. The thick film containing TiO$_2$ shows a lower sensitivity compared to γ-Fe$_2$O$_3$ thick film and this difference is evident at gas concentrations higher than 50 ppm. For γ-Fe$_2$O$_3$ thick film, the active zone (between 5 and 100 ppm) is larger than that of γ-Fe$_2$O$_3$ - TiO$_2$ thick film (between 5 and 50 ppm) due to higher porosity and intergranular coupling.

The response times of γ-Fe$_2$O$_3$ thick film sensor towards various ethanol concentrations (0, 5, 10, 20, 50, 100 and 150 ppm) were also evaluated (Fig. 8). The response time (the time required to reach a new resistance value after the gas

concentration has changed) depends on gas concentration. With increasing ethanol concentration, the response time of the resistance decreased, but it remained within 60–180 seconds. The response times for γ-Fe_2O_3-TiO_2 film towards ethanol were found to be sligthly longer due to lower porosity of this film.
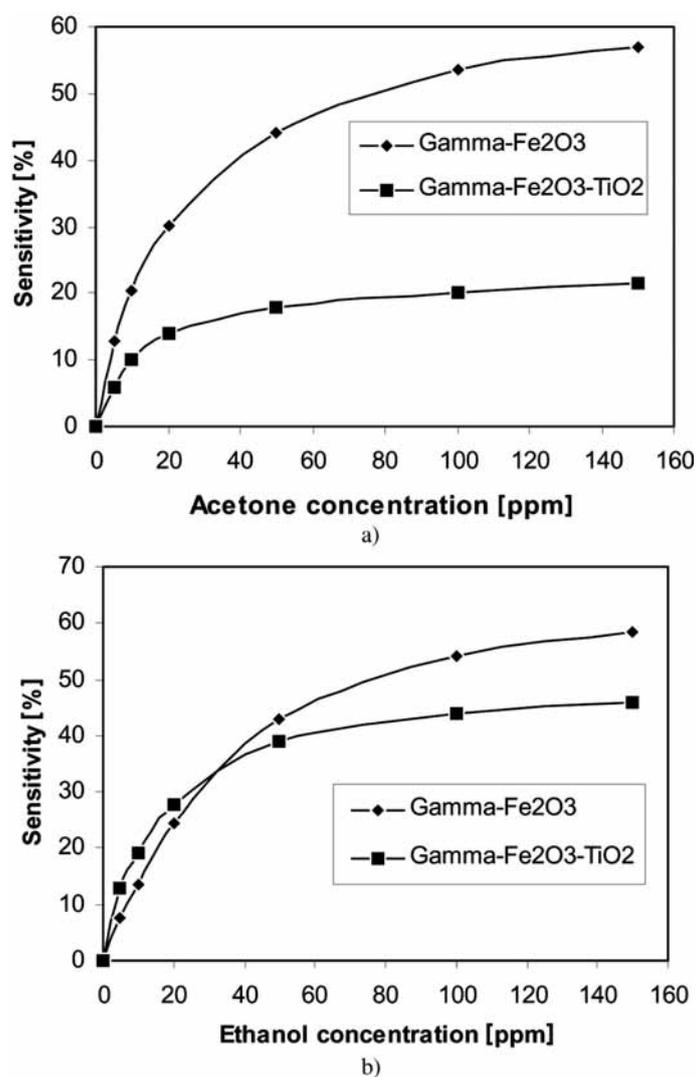

Fig. 7 – Variation of sensitivity with: a) acetone concentration at ope-rating temperature of 330°C; b) ethanol concentration at operating temperature of 310°C, for studied films.
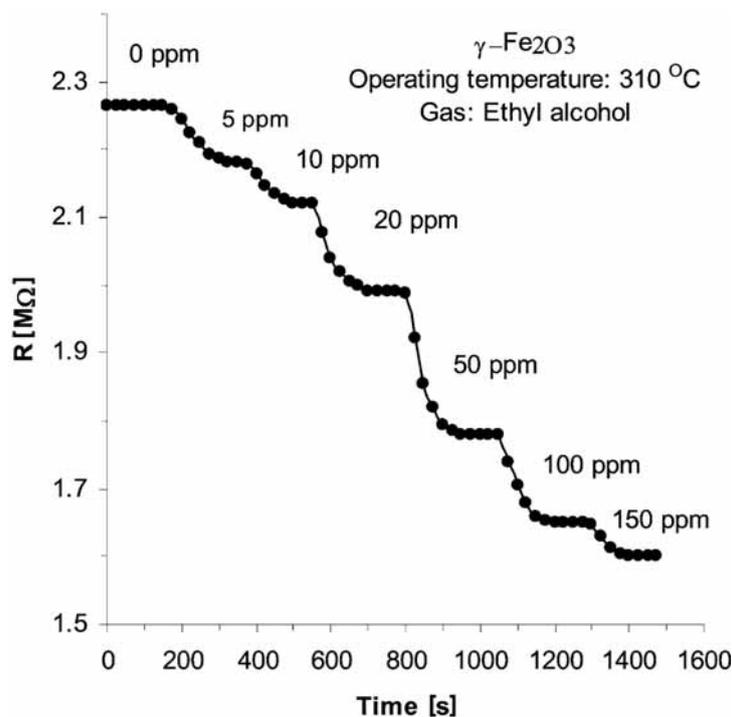
Fig. 8 – Response time of γ-Fe$_2$O$_3$ thick film to various ethyl alcohol concentrations.

4. CONCLUSIONS

Thick films of γ-Fe$_2$O$_3$ without and with TiO$_2$ for gas sensors were fabricated by screen-printing method and their gas sensing characteristics were investigated. γ-Fe$_2$O$_3$ was obtained by thermal decomposition of ferric oxalate. The sensitivity to acetone, ethanol, ammonia and LPG gas was studied. γ-Fe$_2$O$_3$ thick film is sensitive to ethanol, ammonia and acetone and less sensitive to LPG. γ-Fe$_2$O$_3$-TiO$_2$ thick film shows a smaller gas sensitivity. The adition of TiO$_2$ determines a selective sensitivity to ethanol by decreasing the sensitivity to the other reducing gases. The poorer intergranular coupling and the lower porosity can explain the lower sensitivities of γ-Fe$_2$O$_3$-TiO$_2$ thick film compared to γ-Fe$_2$O$_3$ thick film.

With increasing gas concentration from 5 to 150 ppm the gas sensitivity increases whereas the response time of the film resistance decreases, but it remained within 60–180 seconds.

Unfortunately, these films do not have a very high sensitivity. These results are preliminary. Further investigations are necessary to improve the sensitivity of

γ-Fe$_2$O$_3$-TiO$_2$ film to ethanol and to establish the role of TiO$_2$ in selective detection of the ethanol.

REFERENCES

1. M. Aslam, V. A. Chaudhary, I. S. Mulla, S. R. Sainkar, A. B. Mandale, A. A. Belhekar, K. Vijayamohanan, *A highly selective ammonia gas sensor using surface-ruthenated zinc oxide*, Sensors and Actuators B Chemical, **75**, 162–167 (1999).
2. N. Yamamoto, *The effect of reducing gases on the conductivities of metal oxide semiconductors*, Japanese Journal Applied Physics, **20**, 721–726 (1981).
3. N. Rezlescu, C. Doroftei, E. Rezlescu, P. D. Popa, *The influence of Sn^{4+} and/or Mo^{6+} ions on the structure, electrical and gas sensing properties of Mg-ferrite*, Physica Status Solidi, A **203**, 306–316 (2006).
4. N. Rezlescu, N. Iftimie, E. Rezlescu, C. Doroftei, P. D. Popa, *Semiconducting gas sensor for acetone based on the fine grained nickel ferrite*, Sensors and Actuators B: Chemical, **114**, 427–432 (2006).
5. D. R. Patil, L. A. Patil, G. H. Jain, M. S. Wagh, S. A. Patil, *Surface activated ZnO thick film resistors for LPG gas sensing*, Sensors & Transducers Journal, **74**, 874–883 (2006).
6. H. Arima, A. Ikegami, T. Noro, M. Kaneyasu, *New sity gas detector using thick film hybrid sensor*, in: Proc. 32nd Electronic Components Conference, 1982, pp. 290–295.
7. Z. Jin, H. J. Zhou, Z. L. Jin, R. F. Savinell, C. C. Liu, *Application of nano-crystalline porous tin oxide thin film for CO sensing*, Sensors and Actuators B: Chemical, **52**, 188–194 (1998).
8. I. Ferreira, R. Igreja, E. Fortunato, R. Martins, *Porous a/nc-Si:H films produced by HW-CVD as ethanol vapour detector and primary fuell cell*, Sensors and Actuators B: Chemical, **103**, 344–349 (2004).
9. A. Ratna Phani, S. Manorama, V. J. Rao, *Effect of additive on the response of sensors utilizing semiconducting oxide on carbon monoxide sensitivity*, Applied Physics Letters, **66**, 3489–3491 (1995).
10. K. I. Ganasekar, B. Rambabu, K. Lanery, *Role of grain boundaries in exceptionally H$_2$ sensitive highly oriented laser ablated thin films of SnO$_2$*, J. Electrochem. Soc., **149**, 1119–1125 (2002).
11. G. Zang, M. Liu, *Effect of particle size and dopant on properties of SnO$_2$-based gas sensor*, Sensors and Actuators B: Chemical, **69**, 144–152 (2000).
12. A. Gurlo, N. Barsan, U. Weimar, *Mechanism of NO$_2$ Sensing on SnO$_2$ and In$_2$O$_3$ Thick Film Sensors as Revealed by Simultaneous Consumption and Resistivity Measurements*, in: The 16th European Conference on Solid-State Transducers, September 15–18, 2002, Prague, Czech. Republic, pp. 970–973.
13. T. G. G. Maffeis *et al.*, *Nano-crystalline SnO$_2$ gas sensor response to O$_2$ and CH$_4$ at alevated temperature investigated by XPS*, Surface Science, **520**, 29–34 (2002).
14. R. Martins, E. Fortunato, P. Nunes, I. Fereira, A. Marques, *Zinc oxide as an ozone sensor*, Journal of Applied Physics, **96**, 1398–1408 (2004).
15. J. Ding, T. J. McAvoy, R. E. Caviechi, S. Semancik, *Surface state trapping models for SnO$_2$ based microhotplate sensors*, Sensors and Actuators, B **77**, 597–602 (2001).
16. D. D. Lee, D. H. Choi, *Thick-film hydrocarbon gas sensors*, Sensors and Actuators, B **1**, 231–235 (1990).
17. S. Collyer, N. W. Grimes, D. J. Vaughan, G. Longworth, American Mineralogist, **73**, 153–157 (1988).
18. H. Hosono, Z.. Zhang, Y. Abe, *Porous glass-ceramic in the CaO-TiO$_2$-P$_2$O$_5$ system*, J. Amer. Ceram. Society, **52**, 1587–1590 (1989).